Experimental validation of a centrifugal double pendulum vibration absorber model

Vincent Mahé, Alexandre Renault, Aurelien Grolet, Hervé Mahé, Olivier Thomas

Experimental validation of a centrifugal double pendulum vibration absorber model

V. Mahé[a,b], A. Renault[b], A. Grolet[a], H. Mahé[b] and O. Thomas[a]

[a]Arts et Metiers Institute of Technology, LISPEN, HESAM Université, 8 bd. Louis XIV, Lille, 59046, France
[b]Valeo Transmissions, Centre d'Étude des Produits Nouveaux, Espace Industriel Nord, Route de Poulainville, Amiens, 80009, France

ARTICLE INFO

Keywords:
centrifugal double pendulum vibration absorber
experimental analysis
nonlinear dynamics
torsional vibration
nonlinear antiresonance detuning

Abstract

This article deals with the experimental validation of a theoretical model describing the dynamics of a special class of centrifugal pendulum vibration absorbers, designed to reduce the torsional vibrations of rotating machines. The original architecture proposed in this work consists in cylindrical-shaped masses rolling onto each other and acting as double pendulum absorbers. The main interest of these double pendulums lies in the two antiresonances they generate on the main system, which allow to reduce the vibrations at two harmonic orders, unlike standard single pendulum absorbers. The measurements are conducted on an architecture with six double pendulums. They focus on the first rotor antiresonance in the linear and nonlinear regimes, and they are compared to theoretical results from the literature. To the authors' knowledge, this is the first experimental observation of one of the rotor's torsional antiresonances and the first experimental validation of a double pendulum absorber model.

1. Introduction

In the context of reducing polluting emissions and fuel consumption of vehicles using thermal engines, automotive manufacturers are attempting to decrease the cylinder capacity and engine rotational speed. These advancements result in a notable increase in rotational irregularities known as acyclisms, primarily caused by higher combustion pressure. One of the key characteristics of these reciprocating engines is the proportionality relation between the acyclism frequency and the engine rotational speed. The coefficient that determines this relationship is known as the engine order and is solely dependent on the engine's design. During an acceleration phase, the engine covers a wide range of frequencies that include various driveline torsional modes. This situation can lead to significant levels of noise and vibration inside the passenger compartment, as well as premature wear of the driveline components.

Centrifugal pendulum vibration absorbers (CPVAs) are a mean to mitigate the torsional vibrations of driveline components. They consist in masses (pendulums) oscillating relatively to a primary inertia (rotor), hence generating a torque on the latter that balances with an external acyclic torque. The present study focuses on centrifugal double pendulum vibration absorbers (CDPVAs), whose operational principle is the same as that of CPVAs, except that double pendulums are used instead of simple ones. These pendulum absorbers are driven by the centrifugal acceleration field resulting from the system's rotation, so their natural frequencies are directly proportional to the engine's rotational speed. Therefore, CPVAs and CDPVAs operate as dynamic vibration absorbers tuned to an order (two orders for CDPVAs) rather than a specific frequency. This enables these devices to generate a rotor antiresonance at a given order (two antiresonances for CDPVAs), and the associated antiresonance frequency is proportional to the rotational velocity of the engine, just like the acyclism frequency. The vibrations of the rotor can thus be reduced across the entire engine speed range by tuning the pendulums on harmonics of the exciting torque (simple pendulums are typically tuned on the fundamental harmonic). The pendulums' damping needs to be as small as possible for the antiresonances of the driveline components to be deep. Moreover, it can be shown that this kind of device is able to reduce de vibrations of the driveline independently of the presence of eventual resonances [1].

It is R. W. Zdanowich and T. S. Wilson who first studied CDPVAs [2]. Their theoretical work focused on a particular double pendulum architecture made of a pin (pendulum 1) rolling in a circular rotor cavity, and a ring (pendulum 2)

vincent.mahe@ec-nantes.fr (V. Mahé); alexandre.renault@valeo.com (A. Renault); aurelien.grolet@ensam.eu (A. Grolet); herve.mahe@valeo.com (H. Mahé); olivier.thomas@ensam.eu (O. Thomas)
ORCID(s):

whose inner radius rolls on the pin. They showed that these two-degree-of-freedom absorbers have two tuning orders and hence generate two rotor antiresonances.

Then, J.-G. Duh and W. Miao [3] studied a CDPVA whose aim was to reduce the vibrations caused by helicopter rotor blades, which requires the filtering of two distinct orders [4]. In their case, the rotor is not subjected to an acyclic torque but to shaking forces due to the rotor blades that cause translational rotor vibrations. They focused on a design similar to the one proposed in [2] except for a more general shape of the ring, and they showed experimentally the reduction of rotor translational vibrations due to the presence of the CDPVA. CDPVAs exhibit nonlinearities of different natures such as geometric nonlinearities due to the large amplitude of motion of the pendulums, and inertial nonlinearities, for instance due to Coriolis effects and the coupling between the pendulums. J.-G. Duh and M. Wenyong [3] performed a nonlinear analysis showing that overtuning their double pendulum design increases its efficiency at large excitation levels due to the softening behaviour of their CDPVA design.

V. Manchi and C. Sujatha [5] proposed a nonlinear analytical model to represent the dynamical response of a CDPVA made of a single double pendulum. The influence of the pendulums' rotational inertia was not taken into account in that model. A comparison of the analytical results with numerical ones showed a moderate accuracy of the model. The authors also observed experimentally the vibration reduction effect with a CDPVA installed directly on the drive shaft of an automotive vehicle.

V. Mahé *et al.* [6] recently extended previous theoretical works by considering a CDPVA made of two identical double pendulums and by accounting for their rotational inertia. An original tuning strategy based on linear characteristics was proposed to facilitate the design process. Then, a nonlinear analytical model was developed using a strategy similar to those used for CPVAs [7–14]. This CDPVA model allows to capture the nonlinear energy localisation phenomenon, which is an instability of the unison motion that breaks the symmetry of the system by causing the double pendulums to oscillate with different amplitudes and phases (this is a well-known nonlinear phenomenon observed on CPVAs [7, 8, 12, 15–19]). The model developed in [6] also describes the nonlinear antiresonance detuning that occurs as the forcing amplitude is increased. Design guidelines were proposed to improve the filtering performance of CDPVAs and to avoid instabilities of their response. These analytical results were validated numerically.

To the authors' knowledge, the above mentioned works are the only four studies dealing with CDPVAs. Furthermore, only three of them deal with torsional rotor vibrations caused by acyclic torques. Many studies were nevertheless conducted on CPVAs. The reader is referred to [12, 13, 20] for a description of most of these studies. Among the topics of research are the nonlinear jumps of the response (typical of Duffing oscillators [21]), the nonlinear antiresonance detuning, the nonlinear energy localisation phenomenon and the generation of higher rotor harmonics. Among these works, those that include experimental analyses are detailed thereafter.

The vibration reduction effect of CPVAs was observed on helicopters in [22] and on racing cars in [23]. The first comparisons of analytical models of CPVAs' dynamics to experimental data were presented in [24–28]. The response of roller-type pendulums was investigated in [29] and measurements on pendulums tuned to different orders were performed in [30]. The generation of higher rotor harmonics, due to the nonlinear torque exerted by the pendulums, was studied in [30, 31]. The nonlinear antiresonance detuning effect was observed in [31]. This undesired phenomenon causes the antiresonance order to change with the amplitude of the acyclic torque, hence strongly affecting the efficiency of the system. Though CPVAs are usually tuned on the order of the acyclic torque, it is also possible to reduce the rotor's vibrations by tuning the pendulums at half this order. This triggers a subharmonic response that was investigated experimentally in [30, 31]. The localised response of pendulums is another fully nonlinear behaviour that was observed and compared to theoretical predictions in [15]. Most of the works on CPVAs deal with their periodic response, but the case of the transient was investigated experimentally in [32, 33]. Studies focusing on friction issues were conducted in [34, 35] while an analytical and experimental investigation dealing with the slipping of the pendulums was carried out in [31]. Experimental observations of the vibration reduction of CPVAs mounted on recent automotive vehicles were presented in [36, 37].

Among all the works described above, none proposes a comparison of theoretical and experimental results dealing with the torsional vibrations of a CDPVA. This lack of experimental validation is the first motivation of this paper, which presents a comparison between the theoretical results developed in [6] and measurements on a CDPVA prototype. To this aim, measurements are performed around the first rotor antiresonance in the linear and nonlinear regimes. To the authors' knowledge, this provides the first validation of a CDPVA model. The significant complexity

of the equations describing the dynamic response of a CDPVA (see [6]) makes this experimental validation particularly relevant.

There are currently few CDPVA designs proposed in the literature, and they all have shortcomings. This led to the second motivation of this paper, which is to propose a new and convenient CDPVA architecture. The double pendulum architecture proposed in [2], made of a pin and a ring, does not allow for an easy control of the pendulums' mass and lengths, which are crucial parameters to tune the system as desired [6]. The use of a ring-like mass in [3] facilitates the tuning procedure through an easier control of the mass and length of the second pendulum. However, the authors noted and undesired slipping motion of their pendulums, causing an early wear. The design proposed in [5] makes use of two simple pendulums linked through pivot joints equipped with torsional springs. The pivot joints likely increase friction, hence increasing damping and reducing the vibration filtering. In addition, the presence of springs breaks the previously discussed proportionality relation between the CDPVA tuning frequencies and the rotational velocity of the engine, which prevents an optimal tuning of the system over all engine speeds. In this paper, an original architecture made of cylindrical-shape pendulums is proposed. It allows for an easy control of the pendulums' lengths and their mass ratio and does not involve pivot joints. It is thus easy to tune and limits sources of friction, which are detrimental to the system's efficiency.

This paper is organised as follows. The original CDPVA architecture is presented in section 2, and linked to the theoretical model developed in [6]. This model is summarised in section 3 to help understanding the experimental analysis presented in section 4. The later section first describes the CDPVA prototype and the experimental set-up. Then, experimental results are presented and compared to analytical ones. This paper ends with a conclusion in section 5.

2. Double pendulums' architecture and modelling

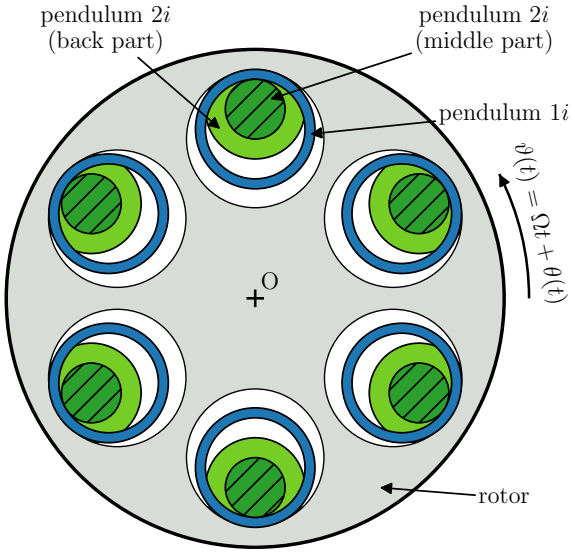

Figure 1: Illustration of the CDPVA architecture proposed in this paper with 6 double pendulums. The front part of the 2nd pendulums is not shown so as not to hide their middle part, which rolling on pendulums 1.

This section presents the CDPVA architecture investigated in this paper. It is depicted in Fig. 1, and a focus on a double pendulum is illustrated in Fig. 2 (different system parameters are used in these two figures to facilitate the visualisation). It is made of a rotor of inertia J_r and $N = 6$ double pendulums. The frame $\mathscr{R}_r(O, \boldsymbol{x_r}, \boldsymbol{y_r}, \boldsymbol{z_0})$ is attached to the rotor at its center O and its rotation with respect to the Galilean frame $\mathscr{R}_0(O, \boldsymbol{x_0}, \boldsymbol{y_0}, \boldsymbol{z_0})$ is $\vartheta(t) = \Omega t + \theta(t)$, where t is the time, Ω is the mean rotational velocity, and $\theta(t)$ corresponds to the fluctuating part of the rotation.

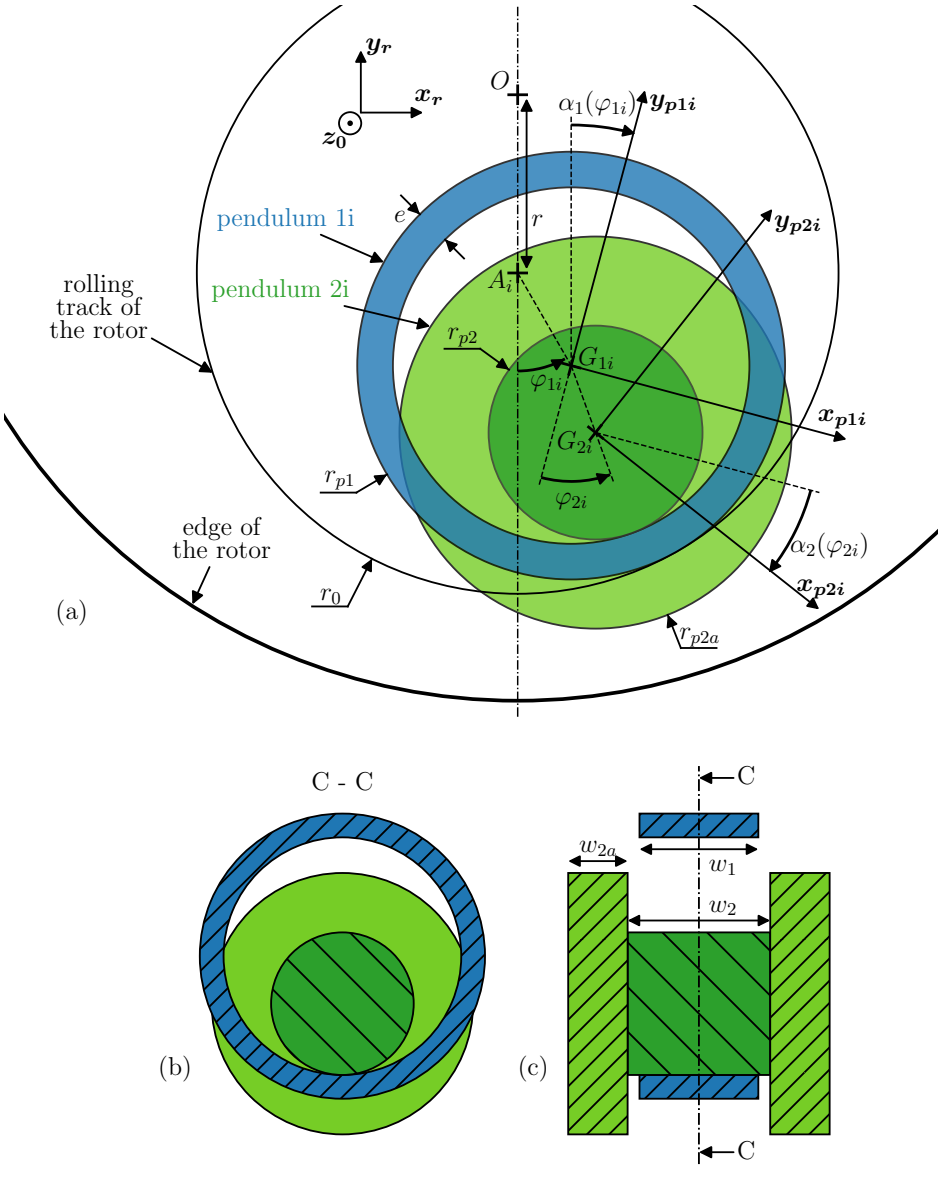

Figure 2: Views of a double pendulum with cylindrical shape pendulums. Front view of a displaced configuration (a), front view (b) and side view (c) in the centrifugated position.

The N identical double pendulums are oscillating relatively to the rotor. Pendulum $1i$ (blue), $i = 1, ..., N$, is a hollow cylinder of centre of mass G_{1i}, external radius r_{p1}, thickness e and width w_1. It rolls on the rotor's rolling track (thin black circle), which is a circular hole of radius r_0 and centre A_i such that $OA_i = r$. The position of G_{1i} with respect to $\mathscr{R}_r$ is located through the angle $\varphi_{1i}(t)$. Note that in practice the rotor's rolling track might not be a full circle due to space requirements, which limits the amplitude of motion of pendulums 1. The frame $\mathscr{R}_{p1i}(G_{1i}, \boldsymbol{x_{p1i}}, \boldsymbol{y_{p1i}}, \boldsymbol{z_0})$ is attached to pendulum 1i at point G_{1i}. Pendulum $2i$, whose centre of mass is G_{2i}, is made of three parts, as can be seen in Fig. 2(c): A cylinder of radius r_{p2} and width w_2 rolls on the inner part of pendulum $1i$. In addition, on each side of this small-radius cylinder are two additional cylinders of radius r_{p2a} and width w_{2a}, giving pendulum $2i$ an H-shape. The purpose of these additional cylinders is to provide an easier control of the mass and inertia of pendulums 2. The position of G_{2i} with respect to $\mathscr{R}_{p1i}$ is located through the angle $\varphi_{2i}(t)$, and the frame $\mathscr{R}_{p2i}(G_{2i}, \boldsymbol{x_{p2i}}, \boldsymbol{y_{p2i}}, \boldsymbol{z_0})$ is attached to pendulum 2 at point G_{2i}.

Note that the double pendulum depicted in Fig. 2 can be seen as a pin-like mass (pendulum 2) rolling in a ring (pendulum 1) which itself rolls on the rotor's track. It is thus the opposite configuration of the one proposed in [2] and [3], where the ring (or ring-like mass) was rolling on a pin, which was itself rolling on the rotor's track.

In order to use the theoretical model developed in [6], one must link the physical pendulums' dimensions to their masses m_1 and m_2, inertias I_1 and I_2, rotations about their centre of mass $\alpha_1(\varphi_{1i})$ and $\alpha_2(\varphi_{2i})$, and paths radii ℓ_1 and ℓ_2. With ρ_1 and ρ_2 the densities of pendulums $1i$ and $2i$, one can write their masses and inertias as

$$\begin{aligned} m_1 &= \rho_1 w_1 \pi (r_{p1}^2 - (r_{p1} - e)^2), \quad I_1 = \frac{1}{2} m_1 (r_{p1}^2 + (r_{p1} + e)^2), \\ m_2 &= \rho_2 w_2 \pi r_{p1}^2 + 2\rho_2 w_{2a} \pi r_{p2a}^2, \quad I_2 = \frac{1}{2} \rho_2 w_2 \pi r_{p1}^4 + \rho_2 w_{2a} \pi r_{p2a}^4. \end{aligned} \tag{1}$$

Their rotation about their centre of mass, corresponding to the rotation of $\mathscr{R}_{p1i}$ with respect to $\mathscr{R}_r$ and that of $\mathscr{R}_{p2i}$ with respect to $\mathscr{R}_{p1i}$, can be derived from the rolling without slipping conditions. This leads to

$$\alpha_1(\varphi_{1i}) = \alpha_{11} \varphi_{1i}, \quad \alpha_{11} = 1 - \frac{r_0}{r_{p1}}, \tag{2a}$$

$$\alpha_2(\varphi_{2i}) = \alpha_{21} \varphi_{2i}, \quad \alpha_{21} = 1 - \frac{r_{p1} - e}{r_{p2}}, \tag{2b}$$

such that the rotations are linear in φ_{1i} and φ_{2i}, respectively. As the rotor's cavity and the rolling components are all circular, the centres of mass of pendulums 1 and 2 follow circular paths with respect to the rotor and pendulums 1, respectively. The radii of these paths are denoted ℓ_1 and ℓ_2 and they can be seen as the virtual lengths of a double pendulum. Their expression as a function of the system's geometry is

$$\ell_1 = r_0 - r_{p1}, \quad \ell_2 = r_{p1} - e - r_{p2}. \tag{3}$$

3. Theoretical background

This section sums up the main theoretical derivations of [6] so as to facilitate the understanding of the experimental analysis presented in section 4.

The motion of the CDPVA is initiated by an external torque $T(\vartheta) = T_0 + T_1 \cos(n\vartheta)$ applied on the rotor. T_0 is the constant part of the torque and T_1 is the amplitude of its first harmonic, of order n. In a thermal engine n corresponds to the number of strikes per rotation of the crankshaft. A linear viscous damping coefficient b_r models the damping between the rotor and the ground. The rotor's damping balances with the constant torque to set the mean rotational velocity $\Omega = T_0/b_r$ while the harmonic torque is the source of the CDPVA's oscillations. Linear viscous damping coefficients b_1 and b_2 are used to model the damping between the rotor and pendulums $1i$ and between pendulums $1i$ and pendulums $2i$, respectively. As discussed in [28] it is difficult to accurately account for the multiple sources of damping of a real system, which is why most theoretical CPVA studies use viscous damping as a simplified representation of all damping mechanisms.

Among the multiple sources of damping, the system can be subject to friction due to (i) the rolling resistance [35, 36], (ii) a planar contact between side surfaces of the pendulums and rotor [35, 38] and (iii) an imperfect rolling without slipping motion [31]. These friction sources are the same as for the widely used bifilar CPVAs. Previous studies successfully compared experimental data of bifilar CPVAs with theoretical models considering only equivalent viscous damping [37]. In a first approximation it is thus relevant to neglect friction in bifilar CPVA models. It was chosen to adopt that assumption in the nonlinear analytical CDPVA model used in the present study for simplicity's sake. The extension of that model to the presence of friction, which could improve the prediction of the system's dynamics, is left for future works.

Assuming small fluctuations of the rotor's rotational velocity, the equations of motion of the CDPVA take the form

$$\boldsymbol{M}\boldsymbol{q}'' + \boldsymbol{C}\boldsymbol{q}' + \boldsymbol{K}\boldsymbol{q} + \boldsymbol{f}_{\text{nl}}(\boldsymbol{q}, \boldsymbol{q}', \boldsymbol{q}'') = \boldsymbol{f}(\vartheta), \tag{4}$$

where $\boldsymbol{q} = [\theta, \varphi_{11}, \dots, \varphi_{1N}, \varphi_{21}, \dots, \varphi_{2N}]^\intercal$ is the vector containing the $1 + 2N$ degree-of-freedom ($^\intercal$ indicates the transpose) and $(\bullet)' = d(\bullet)/d\vartheta$. $\boldsymbol{M}$, $\boldsymbol{C}$, $\boldsymbol{K}$ represent the mass, damping and stiffness matrices, respectively, while $\boldsymbol{f}_{\text{nl}}(\boldsymbol{q}, \boldsymbol{q}', \boldsymbol{q}'')$ and $\boldsymbol{f}(\vartheta)$ are vectors containing nonlinear inertial terms and periodic forcing terms. In the system of $1 + 2N$ equations generated by Eq. (4), the first equation governs the motion of $\theta(\vartheta)$, the next N ones govern the $\varphi_{1i}(\vartheta)$ and the last N equations govern the $\varphi_{2i}(\vartheta)$.

3.1. Linear analysis

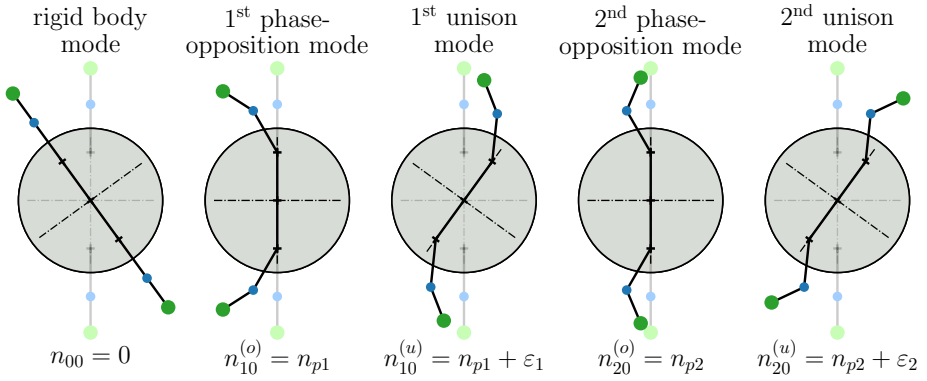

Figure 3: Modes of a CDPVA made of $N = 2$ double pendulums. For $N > 2$ the phase-opposition modes would be degenerated. The rotation of the pendulums about their centre of mass is not represented in this figure. ε_1 and ε_2 indicate that $n_{10}^{(u)}$ and $n_{20}^{(u)}$ are slightly larger than n_{p1} and n_{p2}, respectively.

The linearised equations of motion can be derived from Eq. (4). The five linear modes of a system with $N = 2$ double pendulums are computed in [6] and illustrated in Fig. 3. The eigenorders (analogous to eigenfrequencies) are indicated below each mode shape. n_{p1} and n_{p2} are the tuning orders of the CDPVA and correspond to the two eigenorders of a double pendulum when it is uncoupled from the rotor. Superscripts (o) and (u) refer to phase-opposition and unison motions of the two double pendulums, respectively.

The rigid body mode is associated to a rotation of the rotor with no relative motion of the pendulums. The rotor is a node of the phase-opposition modes, and these are the same as the phase-opposition modes of two uncoupled double pendulums, except for the presence of a null rotor's component. Like for CPVAs, one can expect these phase-opposition modes to become degenerated if a CDPVA with $N > 2$ double pendulums was to be considered [15]. Nevertheless, this degeneracy does not modify the expected response of the system, nor its stability [6]. The unison modes are associated to a unison motion of the double pendulums with at least one of the pendulums oscillating in phase-opposition with respect to the rotor.

The linear forced response of a CDPVA is computed in [6] and yields periodic solutions of the form

$$\ddot{\theta} = H_1 \cos(n\vartheta - \psi_1), \quad \varphi_{1i} = a_1 \cos(n\vartheta - \xi_1), \quad \varphi_{2i} = a_2 \cos(n\vartheta - \xi_2), \quad i = 1, ..., N. \tag{5}$$

The linear response of the prototype investigated experimentally in section 4 is illustrated in Fig. 4, which represents the amplitude response of the rotor (a) and pendulums (b) as a function of the excitation order n. Note that in practice, the excitation order is fixed such that n is a constant and the CDPVA is tuned close from n. Nevertheless, mistuning can exist, either intentionally or because of material imperfections for instance. Varying the excitation order, as in Fig. 4, is similar to introducing mistuning and is therefore relevant for studying the effect of mistuning on the system's response [39]. In addition, the rotor's amplitude with fixed pendulums rather than without pendulums is considered as a reference (black dashed line in Fig. 4(a)) to get rid of any added-mass effect.

The rotor's amplitude, visible in Fig. 4(a), exhibits two antiresonances: one close from $n_{p1} = 1.3$ and the other slightly below n_{p2}, around $n = 7.9$. It is demonstrated in [6] that, in the absence of damping and in the linear regime, the antiresonances are located at n_{p1} and n_{p2}, which is why n_{p1} and n_{p2} are referred to as first and second tuning orders, respectively. This is verified for the first antiresonance in Fig. 4, but not for the second one. This is due to relatively large values of damping coefficients identified in section 4.3, which significantly shifts the second rotor antiresonance to the left and flattens it. With these damping values, if a torque of order n is applied to the rotor, it is thus wise to choose $n_{p1} \approx n$ to significantly reduce the vibration level. If damping was smaller, one could also choose $n_{p2} \approx n$ to filter the vibrations using the second antiresonance. The absorber's performance can be quantified by comparing the rotor's vibrations with fixed and moving pendulums at the two antiresonance orders, as detailed in [6].

The unison response of the pendulums is visible in Fig. 4(b). They respond only on the unison modes because the fluctuating torque is exerted on the rotor, which is a node of the phase-opposition modes, and they are not affected by the rigid body mode.

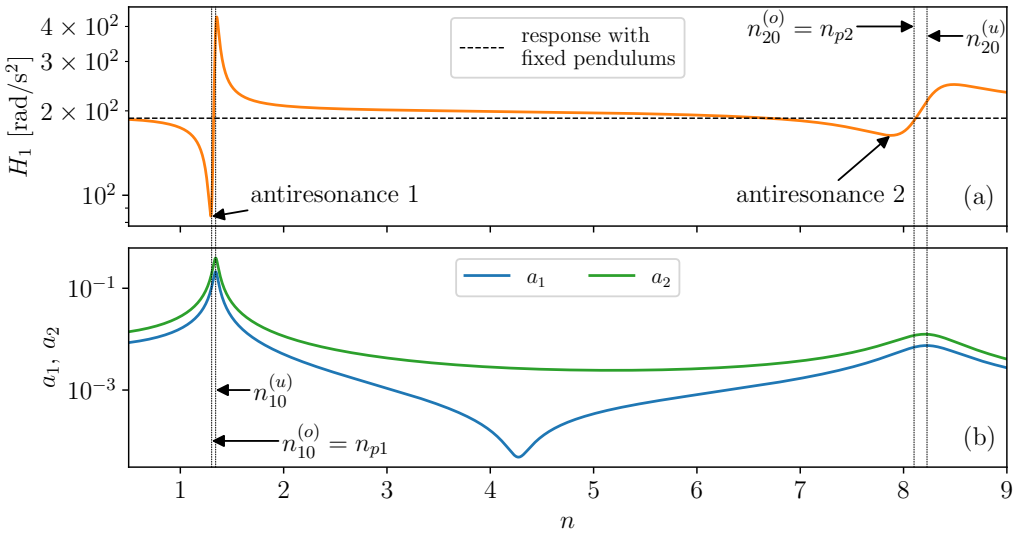

Figure 4: Linear response of the CDPVA prototype investigated experimentally in section 4.3 showing the amplitude response of the rotor (a) and pendulums (b) as a function of the excitation order n. The dashed black line in (a) corresponds to the rotor's response with fixed pendulums. $T_1 = 5$ [Nm], $\Omega = 1500$ [rpm] and the system parameters are given in Tab. 2. The damping coefficients are those identified in section 4.3: $b_1 = b_2 = 50$ [Nm.s] and $b_r = 0.001$ [Nm.s].

3.2. Nonlinear analysis

As discussed in section 1, centrifugal pendulum systems are subjected to various sources of nonlinearities. The proper use of these systems thus requires a nonlinear analysis of their dynamic behaviour, as previously done in [6]. The developments from that previous work involved in the comparison between analytical and experimental results (section 4.3) are presented thereafter.

Analytical solutions of Eq. (4) can be derived using the method of multiple scales, leading to a rotor's response with a fundamental harmonic of the form $\ddot{\theta}^{(1)} = H_1 \cos(n\vartheta - \psi_1)$. The amplitude H_1 and phase ψ_1 are given in [6] as a function of the excitation order n and torque level T_1 and are not recalled here given the complexity of their expressions. In the present paper, a small adjustment had to be made regarding the amplitude H_1 in order to increase the accuracy of the analytical solutions and obtain a better matching between analytical and experimental results in section 4.3. Indeed, in [6], the dimensionless parameter

$$\mu = \frac{N\left(m_1(r+\ell_1)^2 + m_2(r+\ell_1+\ell_2)^2\right)}{J_r + N(I_1+I_2)} \tag{6}$$

representing the ratio of the double pendulums' geometric inertia over the rotational inertia of the CDPVA was assumed small enough to use the approximation $(1+\mu)\theta'' \approx \theta''$. This allowed the application of perturbation methods, but in the present paper $\mu = 0.323$ (this is computed from Tab. 2) is relatively large so this approximation is a source of noticeable inaccuracies. To remedy this, we simply redefine the first harmonic amplitude of rotor's acceleration derived in [6] as $H_1 \to H_1/(1+\mu)$.

The nonlinear antiresonance detuning is a phenomenon studied in [6] that will be observed in section 4.3. It corresponds to a shift of the antiresonance orders $n_{\mathrm{AR}i}$, $i = 1, 2$, with respect to the forcing amplitude, such that $n_{\mathrm{AR}i} = n_{pi} + f_{\mathrm{AR}i}(T_1)$. In practice, one would want to avoid this dependency on T_1 as it detunes the CDPVA, thus decreasing its filtering efficiency. A design rule was proposed in [6] to choose the system parameters so as to prevent this nonlinear detuning.

r	r_0	r_{p1}	w_1	e	r_{p2}	w_2	r_{p2a}	w_{2a}
60	25.5	15.49	15	3	8.45	18	19	8

Table 1
Geometric parameters of the prototype (all in [mm]).

4. Experimental analysis

This section presents the experimental analysis carried out in this work. Section 4.1 describes the CDPVA prototype while the experimental set-up is detailed in section 4.2. The experimental results are discussed in section 4.3 and compared to analytical derivations.

4.1. CDPVA prototype

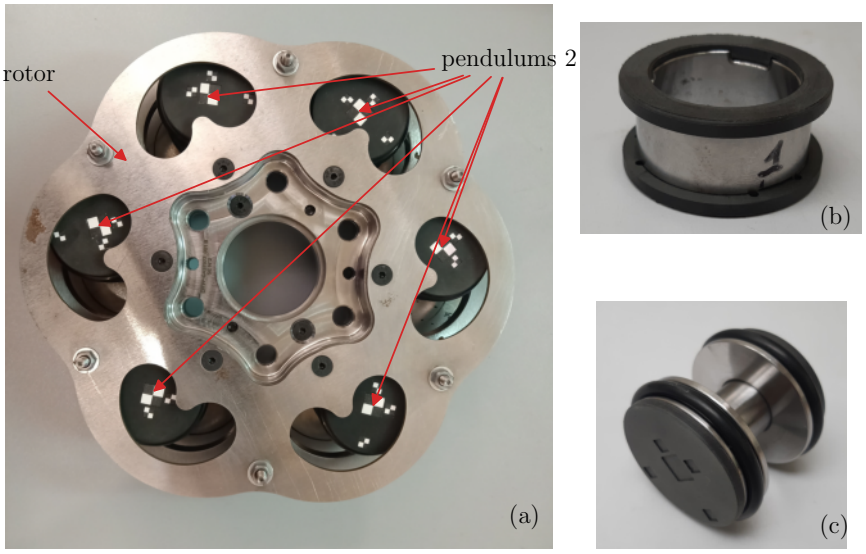

Figure 5: CDPVA used for the experiments (a). Pendulums 1 (b) are hollow cylinders and pendulums 2 (c) are made of a small-radius cylinder rigidly linked to two larger cylinders, whose aim is to control the mass and inertia. Pendulums 1 are hidden behind pendulums 2 in (a).

The CDPVA prototype investigated in this paper is shown in Fig. 5(a). It is made of a rotor and six double pendulums whose first and second pendulums are shown in Fig. 5(b) and (c), respectively. The pendulums are mainly made of steel, but they also include plastic stoppers (in black) whose role it to prevent steel/steel friction and shocks. Friction and shocks are not desired but they are likely to occur when the system starts (the pendulums go from rest to their centrifugated position) and stops (the pendulums go back to their rest position). Shocks may also occur when the pendulums hit the end of their path. The daisy-shape of the rotor allows to reduce its inertia. The design of this prototype is slightly more complicated than the architecture presented in section 2, where perfectly cylindrical pendulums made of a single material are considered. Nevertheless, this simplified representation remains accurate enough to substantially fasten the design process, and a detailed finite element model can be used in the last design stage for an optimal choice of the system's parameters.

The geometric parameters of the prototype are given in Tab. 1 and the parameters of the prototype useful to the analytical developments discussed in section 3 are given in Tab. 2. Note that m_1 and m_2 were not computed from Eq. (1) (which yields values of 31.05 [g] and 174.14 [g], respectively), but were measured on the real system. However, the values used for I_1 and I_2 are those computed from Eq. (1) as they were difficult to measure and lead to good fittings between the theoretical model and the experiments (*cf.* section 4.3). With these parameters, the tuning orders of the CDPVA are $n_{p1} = 1.3$ and $n_{p2} = 8.1$.

N	r [mm]	ℓ_1 [mm]	ℓ_2 [mm]	m_1 [g]	m_2 [g]	I_1 [g.m^2]	I_2 [g.m^2]	J_r [g.m^2]	α_{11}	α_{21}
6	60	10.01	4.04	30.85	169.55	0.006147	0.02684	11.373	-0.646	-0.478

Table 2
Parameters of the prototype useful to the analytical developments summarised in section 3.

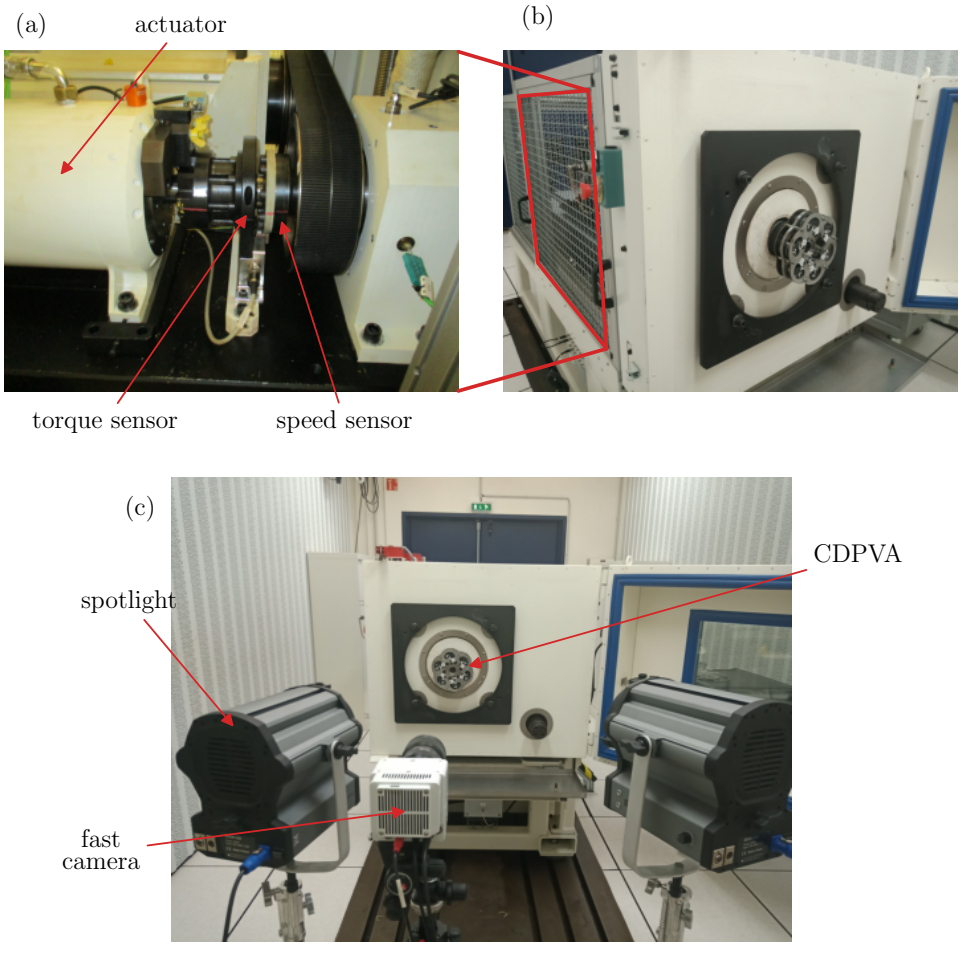

Figure 6: Experimental set-up.

4.2. Experimental set-up

The experimental set-up is shown in Fig. 6. The rotor is fixed on the rotating shaft of a test-bed, whose inertia is J_s. The inertia J_r thus has to be replaced by the equivalent inertia $J_{\text{eq}} = J_r + J_s$ in the model developed in [6] and summarised in sections 3.1 and 3.2.

The procedure to obtain the amplitude of the first rotor harmonic H_1 as a function of the excitation order n for different forcing amplitudes is explained thereafter. Sweeps with respect to n are performed and the time signal of the rotor's velocity is measured. Its acceleration is computed using numerical differentiation and the amplitude of its first harmonic as a function of the excitation order is obtained using a sliding discrete Fourier transform. When performing a sweep, the system was first centrifugated (i.e. a rotational speed Ω is chosen but no fluctuating torque is applied). Note that in practice, when the test-bed receives an input Ω, it adjusts the constant part of the torque T_0 using the data

measured by the torque and speed sensors, a control loop and the actuator until it reaches the rotational velocity Ω. When the desired rotational velocity is reached, a fluctuating torque of amplitude T_1 and order n is applied. The sweep is initiated once the steady-state is established by specifying a value of n to reach and a time Δt to attain this value. Large Δt were used so that the sweeps were performed slowly enough to be similar to a succession of steady states.

4.3. Experimental results

The experimental results are now presented and compared to the analytical model developed in [6]. The parameters of that model are all known (torque, mean rotational velocity, masses, inertias, lengths) except for the pendulums' viscous damping coefficients, which are determined as follows. First, for simplicity's sake, the two pendulums' coefficients are assumed equal. The inaccuracies arising from this hypothesis are limited since the two coefficients should, a priori, be of the same order of magnitude. Then, the viscous damping coefficient is adjusted such as to obtain the best fit between the experimental and analytical results around the antiresonance. The antiresonance is chosen as it is the most damping-sensitive point of the response, together with the resonance. Moreover, it would be ill-advised to use the resonance for damping identification as (i) large pendulums' amplitude increases the odds of slipping (this is discussed further thereafter) and (ii) nonlinear effects such as jumps of the response complicate the measurements around the resonance.

The experimental results are illustrated and compared to analytical ones in Fig. 7, which depicts the amplitude response of the first rotor harmonic around its first antiresonance in the linear (a) and nonlinear (b) regimes.

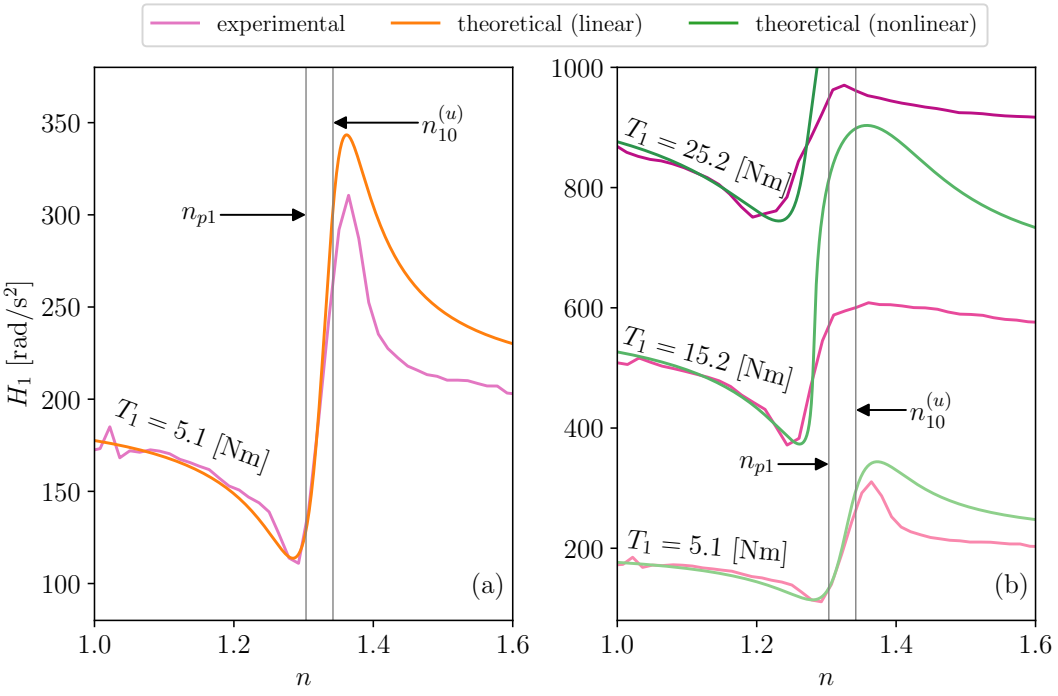

Figure 7: Amplitude of the first harmonic of the rotor's acceleration around the first antiresonance in the linear regime (a) and the nonlinear regime (b). Pink curves correspond to measurements while the theoretical results obtained through the linear and nonlinear models of [6] are shown in orange and green, respectively. Responses for several torque levels are presented in (b), where darker lines are associated to larger torque levels. The rotational velocity is $\Omega = 1000$ [rpm]. The pendulums' damping coefficients used in (a) are $b_1 = b_2 = 50$ [Nm.s] and the ones used in (b) are $b_1 = b_2 = \{70, 80, 135\}$ [Nm.s] for the responses at $T_1 = \{5.1, 15.2, 25.2\}$ [Nm], respectively. The rotor's damping is $b_r = 0.001$ [Nm.s].

The comparison in the linear regime shows a good fitting, thus validating the linear solution derived in [6]. The relatively large pendulums' damping coefficients identified slightly shift the antiresonance order to the left of the tuning order n_{p1}, as predicted by the linear model. For the same reason, the resonance order is slightly larger than $n_{10}^{(u)}$. The rotor's damping is related to the mean torque and the rotational velocity such that $T_0 = b_r\Omega$ (*cf.* section 3), from what we deduced $b_r \approx 0.001$ [Nm.s]. There is a small amplitude difference at the resonance which is probably due to the fact

that the order sweep was done slightly too quickly, so there are not enough points on the experimental curve after using the sliding Fourier transform to accurately describe the resonance. The difference in amplitude after the resonance is significant, though not yet well understood. It could be related to a slipping motion of the pendulums triggered when their amplitude increases as they approach the resonance. This slipping motion could persist after the resonance if the sweeps are not performed slowly enough. This hypothesis is discussed further later.

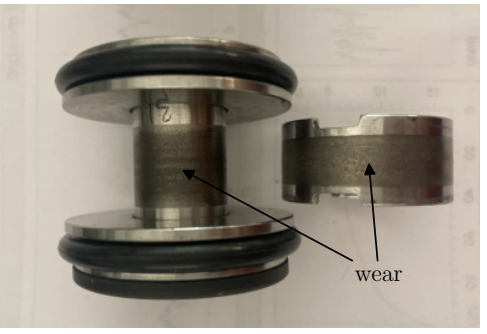

Figure 8: Surface condition of the two pendulums of a double pendulum after the measurements. The inner surface of the first pendulum is not shown here. The shiny surfaces are in perfect condition while the dark grey surfaces were subjected to significant wear.

The nonlinear evolution of the first rotor antiresonance with the torque level is compared to the analytical results of [6] in Fig. 7(b). The nonlinear antiresonance detuning, visible through a shifting of the antiresonance towards lower orders as the torque increases, is relatively well captured by the analytical model. Like in the linear regime, the response at and after the resonance is lower than expected. The increased pendulums' damping values identified as the forcing increases (indicated in the caption of Fig. 7) tend to corroborate the hypothesis of pendulum slipping. Indeed, when slipping occurs it is one of the main damping mechanisms, and it is favoured by large oscillation amplitudes [31].

The significant wear accumulated during the measurements is visible in Fig. 8, which presents the surface condition of a double pendulum after the measurements, and suggests significant slipping motions. A detailed study of the occurrence of slipping was proposed in [31] for a CPVA. It would be interesting to conduct a similar analysis on a CDPVA in future works. Note that wear was already problematic in a previous CDPVA study dealing with the vibration mitigation of shaking forces [3].

Note that it was proposed in [6] to prevent the nonlinear antiresonance detuning through the nonlinear part of the rotation functions α_1 and α_2. However, with the current architecture, these rotation functions are linear (*cf.* Eq. (2)), so they cannot be used to control the nonlinear tuning of the CDPVA. Another way of controlling the nonlinear tuning of the system is through the shape of the pendulums' paths. ℓ_1 and ℓ_2 would thus no longer be constants but functions of φ_{1i} and φ_{2i}, respectively. This is an interesting way of improving the CDPVA design presented in Fig. 2, and it was used in [31] to control the nonlinear tuning of a CPVA with ball-shape pendulums. The simplest upgrade of this CDPVA design would have rotor tracks with a general (non-circular) shape so the nonlinear tuning of the CDPVA could be controlled through the path of pendulums 1. Using a non-circular inner shape of pendulums 1 to control the path of pendulums 2 seems much more complicated to achieve in practice and is not necessary as it is only an additional nonlinear tuning option. The theoretical and experimental investigation of such an improved CDPVA design is left for future works.

The second antiresonance is not investigated in this study as the test-bed cannot operate at large orders due to its limited frequency band. Nevertheless, the locus of these two antiresonances is not independent [6], so that the validation of the theoretical results around the first antiresonance suggests that these results are also correct around the second antiresonance. Still, this will have to be verified in future works.

5. Conclusion

This paper presents the first experimental investigation and comparison with theoretical developments of the linear and nonlinear dynamic response of a CDPVA subject to a fluctuating torque. These passive absorbers generate two antiresonances, hence reducing the torsional vibrations of a rotating machine at two orders over its whole speed

range. An original CDPVA architecture made of cylindrical-shape double pendulums was first presented. Its tuning parameters are easy to control and it does not involve pivot joints, thus limiting sources of damping and maximising the filtering efficiency. Then, some theoretical background derived in a former study was summarised to provide a basic understanding of the system's dynamics, thereby facilitating the understanding of the experimental analysis presented next. Experiments were conducted on a CDPVA prototype made of six double pendulums. Measurements of the rotor's response around its first antiresonance were performed in the linear and nonlinear regimes and compared to theoretical results. The linear antiresonance was observed were expected, and its nonlinear detuning as the torque amplitude increases was well predicted by the model. These experimental results hence allowed the first experimental validation of a theoretical CDPVA model. The viscous damping coefficients identified experimentally were larger than expected. This can be due to the significant wear of the double pendulums during the tests, probably caused by large pendulums' motion around the resonance that induced slipping. Future works should focus on the analysis of the pendulums' slipping to identify the parameters that could help limiting it. Moreover, additional theoretical studies are necessary to model a CDPVA whose pendulums follow non-circular paths. This would allow to design an upgraded version of the architecture described in this paper that could be nonlinearly tuned and hence prevent the nonlinear antiresonance detuning, which is detrimental to vibration filtering.

CRediT authorship contribution statement

: Vincent MAHE: Formal analysis, Investigation, Validation, Visualisation, Writing - original draft, Methodology, Software. Alexandre RENAULT: Supervision, Resources, Investigation, Methodology, Writing - Review and Editing, Software. Aurélien GROLET: Supervision, Visualisation, Writing - Review and Editing. Hervé MAHE: Supervision, Resources. Olivier THOMAS: Supervision, Visualisation, Writing - Review and Editing.

References

[1] M. Auleley, C. Giraud-Audine, H. Mahé, O. Thomas, Tunable electromagnetic resonant shunt using pulse-width modulation, Journal of Sound and Vibration 500 (2021) 116018. doi:10.1016/j.jsv.2021.116018.

[2] R. W. Zdanowich, T. S. Wilson, The elements of pendulum dampers, Proceedings of the Institution of Mechanical Engineers 143 (1) (1940) 182–210. doi:10.1243/PIME_PROC_1940_143_028_02.

[3] J.-G. Duh, W. Miao, Development of monofilar rotor hub vibration absorber, Tech. rep. (1983).

[4] C. Shi, R. G. Parker, S. W. Shaw, Tuning of centrifugal pendulum vibration absorbers for translational and rotational vibration reduction, Mechanism and Machine Theory 66 (2013) 56–65. doi:10.1016/j.mechmachtheory.2013.03.004.

[5] V. Manchi, C. Sujatha, Torsional vibration reduction of rotating shafts for multiple orders using centrifugal double pendulum vibration absorber, Applied Acoustics 174 (2021) 107768. doi:10.1016/j.apacoust.2020.107768.

[6] V. Mahé, A. Grolet, A. Renault, H. Mahé, O. Thomas, Dynamic stability and efficiency of centrifugal double pendulum vibration absorbers, Mechanism and Machine Theory 197 (2024) 105649. doi:10.1016/j.mechmachtheory.2024.105649.

[7] C.-P. Chao, C.-T. Lee, S. Shaw, Non-unisson dynamics of multiple centrifugal pendulum vibration absorbers, Journal of Sound and Vibration 204 (5) (1997) 769–794. doi:10.1006/jsvi.1997.0960.

[8] C.-P. Chao, S. W. Shaw, C.-T. Lee, Stability of the Unison Response for a Rotating System With Multiple Tautochronic Pendulum Vibration Absorbers, Journal of Applied Mechanics 64 (1) (1997) 149–156. doi:10.1115/1.2787266.

[9] C.-P. Chao, S. W. Shaw, The effects of imperfections on the performance of the subharmonic vibration absorber system, Journal of Sound and Vibration 215 (5) (1998) 1065–1099. doi:10.1006/jsvi.1998.1634.

[10] C.-P. Chao, S. W. Shaw, The dynamic response of multiple pairs of subharmonic torsional vibration absorbers, Journal of Sound and Vibration 231 (2) (2000) 411–431. doi:10.1006/jsvi.1999.2722.

[11] S. W. Shaw, B. Geist, Tuning for Performance and Stability in Systems of Nearly Tautochronic Torsional Vibration Absorbers, Journal of Vibration and Acoustics 132 (4) (2010) 041005. doi:10.1115/1.4000840.

[12] V. Mahé, A. Renault, A. Grolet, H. Mahé, O. Thomas, On the dynamic stability and efficiency of centrifugal pendulum vibration absorbers with rotating pendulums, Journal of Sound and Vibration 536 (2022) 117157. doi:10.1016/j.jsv.2022.117157.

[13] V. Mahe, A. Renault, A. Grolet, H. Mahe, O. Thomas, Subharmonic centrifugal pendulum vibration absorbers allowing a rotational mobility, Mechanical Systems and Signal Processing 177 (2022) 109125. doi:10.1016/j.ymssp.2022.109125.

[14] V. Mahé, A. Renault, A. Grolet, H. Mahé, O. Thomas, On the stability of pairs of subharmonic centrifugal pendulum vibration absorbers allowing a rotational mobility, Nonlinear Dynamics (2023) 17859–17886doi:10.1007/s11071-023-08828-6.

[15] V. Mahe, A. Renault, A. Grolet, O. Thomas, H. Mahe, Dynamic stability of centrifugal pendulum vibration absorbers allowing a rotational mobility, Journal of Sound and Vibration 517 (2022) 116525. doi:10.1016/j.jsv.2021.116525.

[16] M. Cera, M. Cirelli, E. Pennestrì, P. P. Valentini, Design analysis of torsichrone centrifugal pendulum vibration absorbers, Nonlinear Dynamics 104 (2) (2021) 1023–1041. doi:10.1007/s11071-021-06345-y.

[17] J. S. Issa, S. W. Shaw, Synchronous and non-synchronous responses of systems with multiple identical nonlinear vibration absorbers, Journal of Sound and Vibration 348 (2015) 105–125. doi:10.1016/j.jsv.2015.03.021.

[18] A. S. Alsuwaiyan, S. W. Shaw, Non-synchronous and Localized Responses of Systems of Identical Centrifugal Pendulum Vibration Absorbers, Arabian Journal for Science and Engineering 39 (12) (2014) 9205–9217. doi:10.1007/s13369-014-1464-1.

[19] V. Mahé, A. Renault, A. Grolet, H. Mahé, O. Thomas, The localised response and filtering performance of centrifugal pendulum vibration absorbers allowing a rotational mobility, Journal of Sound and Vibration 571 (2024) 118028. doi:10.1016/j.jsv.2023.118028.

[20] K. Nishimura, T. Ikeda, Y. Harata, Localization phenomena in torsional rotating shaft systems with multiple centrifugal pendulum vibration absorbers, Nonlinear Dynamics 83 (3) (2016) 1705–1726. doi:10.1007/s11071-015-2441-2.

[21] I. Kovacic, M. J. Brennan, The Duffing Equation: Nonlinear Oscillators and Their Behaviour, John Wiley & Sons, 2011. doi:10.1002/9780470977859.

[22] M. A. Wachs, The Main Rotor Bifilar Absorber and Its Effect on Helicopter Reliability/Maintainability, in: National Aerospace Engineering and Manufacturing Meeting, 1973, p. 730894. doi:10.4271/730894.

[23] M. Albright, T. Crawford, F. Speckhart, Dynamic Testing and Evaluation of the Torsional Vibration Absorber, in: SAE Technical Paper 942519, SAE International, 1994, p. 8. doi:10.4271/942519.

[24] T. M. Nester, Experimental investigation of circular path centrifugal pendulum vibration absorbers, Master's thesis, Michigan State University, Michigan (2002).

[25] T. M. Nester, A. G. Haddow, S. W. Shaw, Experimental Investigation of a System With Multiple Nearly Identical Centrifugal Pendulum Vibration Absorbers, in: Volume 5: 19th Biennial Conference on Mechanical Vibration and Noise, Parts A, B, and C, ASMEDC, Chicago, Illinois, USA, 2003, pp. 913–921. doi:10.1115/DETC2003/VIB-48410.

[26] A. G. Haddow, S. W. Shaw, Centrifugal Pendulum Vibration Absorbers: An Experimental and Theoretical Investigation, Nonlinear Dynamics 34 (3/4) (2003) 293–307. doi:10.1023/B:NODY.0000013509.51299.c0.

[27] T. M. Nester, P. M. Schmitz, A. G. Haddow, S. W. Shaw, Experimental observations of centrifugal pendulum vibration absorbers, in: International Symposium on Transport Phenomena and Dynamics of Rotating Machinery, Honolulu (Hawaii), 2004.

[28] S. W. Shaw, P. M. Schmitz, A. G. Haddow, Tautochronic Vibration Absorbers for Rotating Systems, Journal of Computational and Nonlinear Dynamics 1 (4) (2006) 283–293. doi:10.1115/1.2338652.

[29] Y. Ishida, T. Inoue, T. Fukami, M. Ueda, Torsional Vibration Suppression by Roller Type Centrifugal Vibration Absorbers, Journal of Vibration and Acoustics 131 (5) (2009) 051012. doi:10.1115/1.3147124.

[30] B. J. Vidmar, Analysis and Design of Multiple Order Centrifugal Pendulum Vibration Absorbers, Ph.D. thesis, American Society of Mechanical Engineers, Chicago, Illinois, USA (2012).

[31] V. Mahé, A. Renault, A. Grolet, H. Mahé, O. Thomas, Experimental investigation of the direct and subharmonic responses of a new design of centrifugal pendulum vibration absorber, Mechanism and Machine Theory 188 (2023) 105401. doi:10.1016/j.mechmachtheory.2023.105401.

[32] J. Mayet, D. Rixen, H. Ulbrich, Experimental Investigation of Centrifugal Pendulum Vibration Absorbers, in: International Conference on Vibration Problems, Lisbon (Portugal), 2013.

[33] R. J. Monroe, S. W. Shaw, Nonlinear Transient Dynamics of Pendulum Torsional Vibration Absorbers—Part I: Theory, Journal of Vibration and Acoustics 135 (1) (2013) 011017. doi:10.1115/1.4007561.

[34] B. J. Vidmar, B. F. Feeny, S. W. Shaw, A. G. Haddow, B. K. Geist, N. J. Verhanovitz, The effects of Coulomb friction on the performance of centrifugal pendulum vibration absorbers, Nonlinear Dynamics 69 (1) (2012) 589–600. doi:10.1007/s11071-011-0289-7.

[35] E. R. Gomez, I. L. Arteaga, L. Kari, Normal-force dependant friction in centrifugal pendulum vibration absorbers: Simulation and experimental investigations, Journal of Sound and Vibration 492 (2021) 115815. doi:10.1016/j.jsv.2020.115815.

[36] E. R. Gomez, J. Sjöstrand, L. Kari, I. L. Arteaga, Torsional vibrations in heavy-truck powertrains with flywheel attached centrifugal pendulum vibration absorbers, Mechanism and Machine Theory 167 (2022) 104547. doi:10.1016/j.mechmachtheory.2021.104547.

[37] A. Renault, Calcul et optimisation d'absorbeurs pendulaires dans une chaîne de traction automobile [Simulation and optimisation of pendular absorbers for automotive powertrain], Ph.D. thesis, ENSAM, Lille, France (2018).

[38] R. Dragani, M. Sarra, The centrifugal pendulum as a non linear torsional vibration absorber, Meccanica 18 (2) (1983) 67–70. doi:10.1007/BF02128346.

[39] A. Grolet, A. Renault, O. Thomas, Energy Localisation in Periodic Structures: Application to Centrifugal Pendulum Vibration Absorber, in: International Symposium on Transport Phenomena and Dynamics of Rotating Machinery, Maui (Hawaii), 2017.